Time-Selective Sampling Receiver for Interference Rejection

Robert W. Jackson, *Fellow, IEEE*

***Abstract*—The use of time-selective sampling is presented as a way to significantly reduce the effect of large interferers on the sensitivity of receivers operating in a crowded spectrum. The concept assumes a discrete-time analog front end, where large distorted samples are discarded and small undistorted samples are retained for use in estimating the desired message signals. Since the retained samples are not uniform in time, signal processing is a challenge. The signal processing is described in cases in which 1) the frequencies of the interferers are known and 2) the frequencies are not known.**

***Index Terms*—Cognitive radio, interference, interference suppression, intermodulation distortion, nonlinear distortion, nonuniform sampling software-defined radio, sampling receiver.**

I. Introduction

The ideal receiver of the future will be capable of collecting wide swaths of spectrum and then adaptively choosing which parts of it to extract. Such receivers would be necessary to implement the techniques of dynamic spectrum access and cognitive radio [1], [2]. To be fully adaptable, their radiofrequency (RF) stages would minimize fixed filtering, while maintaining the capability of extracting very weak signals in the presence of signals that may be more than 90 dB larger [2].

Normally, the RF input to a receiver passes through a fixed prefilter to remove interferers and is then amplified by a low-noise amplifier (LNA) to boost the signal level above the noise generated in succeeding stages (reconfigurable filters, samplers, and downconverters.) To permit adaptability, the fixed filter must be removed. This makes the receiver susceptible to interferers that mix in the LNA nonlinearities to generate intermodulation products that may then mask a small desired signal. A tunable prefilter can be used, but this adds complexity and loss.

Instead of prefiltering in the frequency domain, we proposed [3] postfiltering in the time domain. In such a receiver, the received signal is sampled after the LNA, and all samples larger than some threshold are discarded under the premise that they have been distorted by the LNA nonlinearity. The retained samples have benefitted by the gain of the LNA, without being distorted by its nonlinearity. Their sample times depend on the interferer zero crossings and are, therefore, not uniform. Reconstituting a signal from a nonuniformly sampled data set has been studied in connection with digital audio [4], geophysics, and radio astronomy. In a related manner, we herein directly extract the magnitude and phase variation of a small message signal from low-distortion samples that contain both the message and the interference.

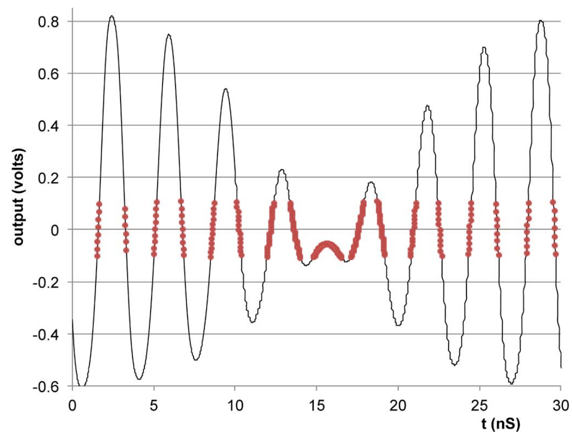

Fig. 1. Plot of LNA output, showing samples taken at small interferer values. The interferers are two sinusoids at 270 and 300 MHz. A third sinusoid, i.e., the message signal, at 240 MHz is too small to be visible.

In a conference brief [3], we described the basic time-selective sampling idea and presented measurements of a simple test case. In Section II, we review the concept. The basic contributions of this brief are described in Sections III and IV, where the message retrieval algorithms are described for cases where the interferer frequencies are known and not well known, respectively. We discuss the effect of noise when too few samples are retained versus distortion when too many are retained.

II. Basic Concept

The input–output relation that approximates a memoryless amplifier below hard saturation is

$$v_o(t) = k_1 v_i(t) + k_2 v_i(t)^2 + k_3 v_i(t)^3 \qquad (1)$$

where v_i is the amplifier input voltage, and v_o is its output. k_1 is determined by the linear gain of the amplifier. k_2 and k_3 depend on the amplifier's second- and third-order intercepts. The second-and third-order terms add distortion at times when v_i is large. In the proposed receiver, the output of the LNA is sampled, but the samples with magnitude greater than some threshold V_T are discarded. The result is a set of sample voltages corresponding to a set of sample times $\Lambda = \{t_n\}$. These samples have gone through a nearly linear amplification since they are small enough to make the nonlinear terms in (1) negligible. Fig. 1 shows a possible output, with the retained sample points marked. Note that, as the interferers become

Manuscript received December 29, 2014; accepted February 26, 2015. Date of publication March 23, 2015; date of current version June 25, 2015. This work was supported in part by the National Science Foundation under Grant ECCS-1201835. This brief was recommended by Associate Editor M. S.-W. Chen.

The author is with the Department of Electrical and Computer Engineering, University of Massachusetts Amherst, Amherst, MA 01003 USA (e-mail: jackson@ecs.umass.edu).

Color versions of one or more of the figures in this brief are available online at http://ieeexplore.ieee.org.

Digital Object Identifier 10.1109/TCSII.2015.2415711

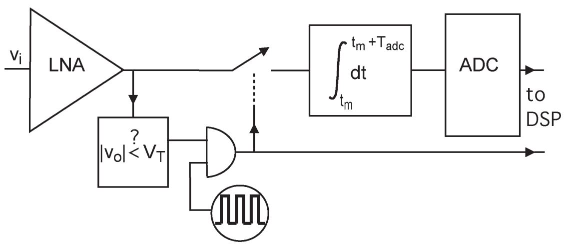

Fig. 2. Conceptual diagram of a receiver for time-selective sampling based on sample size.

larger, there are fewer samples small enough to accept, and this will make it more difficult to detect a message symbol accurately. The accepted samples contain both the interferer and the message, but are not distorted.

In the worst case, the message is much smaller than the interferer. The small message requires the sensitivity provided by an LNA, but the large interferer drives the LNA nonlinearity to create message-blocking sidebands. In such cases, selective sampling is needed. In contrast, when the message and interferer are of similar size, the gain can be set to maintain both sensitivity and low distortion, and all samples can be retained.

Fig. 2 shows a conceptual receiver configuration. The output of the LNA is sampled at a rate set by a sample clock running at a frequency well above the Nyquist rate for the RF signal. However, samples are only taken when the LNA output voltage is below V_T. There will be some cases where there may be many clock cycles between samples, and some cases where many samples will be closely spaced. An integrator is included to accumulate samples (relatively few) over time $T_{\rm adc}$, in order to reduce the required analog-to-digital conversion (ADC) rate. The receiver in Fig. 2 passes to a digital signal processor (DSP) both the integrated samples and a clock pulse when an acceptable sample is taken. In addition, information as to whether the signal v_o is greater than V_T or less than $-V_T$ could be also passed; such information has been shown to aid in sparse signal recovery [4]–[6].

III. Formulation: Known Interferer Spectrum

Signal recovery based on nonuniform sampling has been studied for decades [7]–[11]. Researchers have investigated sampling at user-prescribed pseudorandom times, in order to reduce aliasing effects [10] and in connection with sparse signal assumptions [14]. In contrast to these applications, the location of sample times in our problem *depends on the interference*.

In what follows, the small message signal is recovered by a least mean square (LMS) fit of a signal expansion to the samples sent to the DSP by the ADC in Fig. 2. The formulation recovers the signal's spectral amplitudes and phase directly without reconstituting the full time response. In this section, we assume that the spectral supports of the interferer and message are known.

A. Basic Analysis

Referring to Fig. 2, we assume a uniform sample clock running at a rate f_s, such that, in a block of time $T_{\rm dur}$, the total number of clock pulses is $N_P = T_{\rm dur} f_s$. When the output signal has amplitude $\max(|v_o|) > V_T$, only $N_S < N_P$ samples out of that block are passed on to the integrator. Therefore, N_S is the number of samples in the set $\Lambda = \{t_n\}$. The vector $\mathbf{v}_o = \{v_o(t_n)\}^T$ is the $N_S \times 1$ vector of retained samples.

We also divide the total block time into intervals of duration $T_{\rm ADC}$, each with N_I sample slots. There would be $T_{\rm dur}/T_{\rm ADC} = N_p/N_I$ such intervals. The retained samples in each interval are summed and the output sent to the ADC.

The operation that places the N_S samples in v_o into M_I integrations that make up $v_{\rm ADC}$ can then be described by

$$v_{\rm ADC}(m) = \sum_{n=1}^{N_S} g\left(t_n - mT_{\rm ADC}\right) \cdot v_o(t_n) \tag{2}$$

where $g(\tau) = 1$ for $0 < \tau < T_{\rm ADC}$ and is zero otherwise. (2) can be written in vector form as $\mathbf{v_{ADC}} = \mathbf{G} \cdot \mathbf{v}_o$, where $\mathbf{G}$ is an $M_I \times N_S$ matrix. If every interval had at least one retained sample, then $M_I = N_P/N_I$. Some of the integration intervals will have every sample slot filled, some may have very few filled, and some may have zero samples, depending on V_T, $\max(|v_o|)$, and $T_{\rm ADC}$. In forming $\mathbf{G}$, we eliminate every row corresponding to an interval with zero samples, and thus, $M_I \leq N_p/N_I$. $\mathbf{G}$ is formed in the DSP from the known summation index N_I and the threshold-conditioned clock signal shown in Fig. 2.

In order to recover the entire undistorted output voltage, we assume that it can be represented by a set of sinusoids made up of N_f frequencies $\{\omega_n\}$ plus a dc term, and $t_m \in \Lambda$. Thus

$$v_{\rm oE}\left(t_m\right) = c_0 + \sum_{n=1}^{N_f} \left[c_{Rn} \cos(\omega_n t_m) - c_{In} \sin(\omega_n t_m)\right]. \tag{3}$$

In matrix form, (3) is $\mathbf{v_{oE}} = \mathbf{F} \cdot \mathbf{x} = [1, \mathbf{F}_c, \mathbf{F}_s] \cdot \mathbf{x}$, where the real vector $\mathbf{x} = [c_o, c_{R1}, c_{R2}, \ldots, c_{RN_f}, c_{I1}, c_{I2}, \ldots, c_{IN_f}]^T$ contains the in-phase and quadrature parts of the N_f spectral components. The matrix $\mathbf{F}$ has dimension $N_S \times (2N_f + 1)$ and is made up of a concatenation of a unit column vector and two matrices $(\mathbf{F}_c)_{nm} = \cos(\omega_n t_m)$ and $(\mathbf{F}_s)_{nm} = -\sin(\omega_n t_m)$.

The spectral coefficients $\mathbf{x}$ are estimated by LMS fitting $\mathbf{v}_{\rm oE}$ to $\mathbf{v}_o$, subject to the integration matrix $\mathbf{G}$ and a diagonal weighting matrix $\mathbf{W}$, i.e.,

$$\begin{aligned}\hat{\mathbf{x}} &= \arg\min_x \|\mathbf{W} \cdot \mathbf{G} \cdot (\mathbf{v}_o - \mathbf{v}_{\rm oE})\|_2 \\ &= \arg\min_x \|\mathbf{W} \cdot (\mathbf{v}_{\rm ADC} - \mathbf{G} \cdot \mathbf{F} \cdot \mathbf{x})\|_2\end{aligned} \tag{4}$$

where each weight in $\mathbf{W}$ is the inverse of the number of valid samples in the corresponding integration interval. The integration operation $\mathbf{G}$ reduces the number of measurements in this system from N_S to M_I. We define a measurement matrix $\mathbf{A} = \mathbf{W} \cdot \mathbf{G} \cdot \mathbf{F}$ that has dimension $M_I \times (2N_f + 1)$. Since, in general, $M_I > 2N_f + 1$, we solve for $\hat{\mathbf{x}}$ using a pseudoinverse, i.e.,

$$\hat{\mathbf{x}} = \left(\mathbf{A}^T \cdot \mathbf{A}^{-1}\right) \cdot \mathbf{A}^T \cdot \mathbf{W} \cdot \mathbf{v_{ADC}}. \tag{5}$$

This, then, is an estimate of the spectral amplitudes of both the interferers and the message. The size of $\mathbf{A}^T \cdot \mathbf{A}$ depends on the number of expansion frequencies assumed and not the number of time samples. In cases where the bandwidth is small, the matrix inverse is easily computed. For a larger bandwidth, an iterative approach may be faster [9].

The error vector magnitude (EVM) is defined as EVM $\equiv \|\hat{\mathbf{x}}_m - \hat{\mathbf{x}}_{mo}\| / \|\hat{\mathbf{x}}_{mo}\|$, where $\hat{\mathbf{x}}_m$ is the subset of $\hat{\mathbf{x}}$

corresponding to the retrieved message when the interferer is present, and $\hat{\mathbf{x}}_{mo}$ is the retrieved message with no interferer.

B. Simulated Results: Known Interferers

Here, two cases are presented where the aforementioned analysis is applied. In both cases, the ideal message and interferers are passed through the ideal nonlinear amplifier model described by (1). The power levels and the input-referred third-order intercept point $(\mathrm{IIP3} \equiv 13.3 * k_1/|k_3|\ \mathrm{mW})$ were chosen, such that the intermodulation sidebands bury the message signal, making it impossible to receive without the selective sampling technique.

The first case is a very simple one. A small message tone of -80 dBm is present at 240 MHz, along with two interferers, each with -29 dBm power at 270 and 300 MHz. The amplifier is modeled by 25 dB gain and -9 dBm IIP3 [$k_1 = 18$, $k_3 = -1906\ \mathrm{V}^{-2}$ in (1)]. This choice of interferer and nonlinearity (IIP3) generates a third-order tone on the message frequency at a power level of 11 dB higher than that of the message. Conventional calculation shows that the IIP3 of the amplifier would have to be increased by 15 dB to reduce the intermodulation distortion to a level that produces an EVM less than 10%. Such an increase would require a substantial increase in dc power.

Fig. 3 shows that the EVM drops when a smaller fraction of the total sample set is retained. The sampling frequency was 2 GHz, and the total sample set was $N_p = 5000$ (8 μs). Every eight samples were integrated ($N_I = 8$), and thus, the ADC must convert no faster than 4 ns/sample (250 MHz). The aforementioned analysis was applied with only three expansion frequencies: 240, 270, and 300 MHz and dc [see (3)]. The dashed line is the result when the interferers are 90° out of phase with each other. Its jagged response is due to the changing distribution of $\{t_n\}$ as the threshold drops. If the phase relation between interferers is changed, the curve changes because the points in time, where the interferer drops below the threshold, also change. The solid line averages the EVM for five interferer phase relations. The results show that the error drops below 10%, when less than 45% of the samples are retained for the analysis.

Given a particular interferer, each N_s/N_p fraction can be mapped to a threshold voltage. In Fig. 3, the mapping for the interferer corresponding to the dashed line is shown in the figure axes. For example, when 30% of the samples are taken, the corresponding threshold is 20% of the peak signal voltage.

Fig. 4 shows a second case, which roughly corresponds to the digital television (DTV) white-space problem. A message signal consists of three equal magnitude tones at 293, 294, and 295 MHz, with an average power of -80 dBm. An interferer exists in an adjacent channel at 300 MHz, with a 6-MHz bandwidth and an average power of -8 dBm. The interferer is an 8VSB modulation at a 10.9-MHz symbol rate for an 8-μs duration (brick-wall filter and no pilot.) The interferer peak-to-average ratio is 5–6 dB. The amplifier is modeled as having 10-dBm IIP3. The left inset in Fig. 4 illustrates the input spectrum (log scale), and the right inset illustrates the output spectrum if all samples were retained. The nonlinearity causes shoulders that cover the message signal.

Once again, the plot shows the EVM versus fraction of samples accepted. The sampling frequency is 2 GHz and the total sample set was $N_p = 16\,000$. The integration interval is eight samples ($N_I = 8$). The analysis in part A was applied with expansion frequencies of {0, 293, 294, 295} MHz, plus 105 frequencies extending from 296 to 309 MHz, with 0.125-MHz separation. The algorithm extracts the entire spectrum, but the complex amplitudes of the three message signals are of particular interest. The solid line is the EVM averaged over 100 possible choices of interferer sequence. The EVM

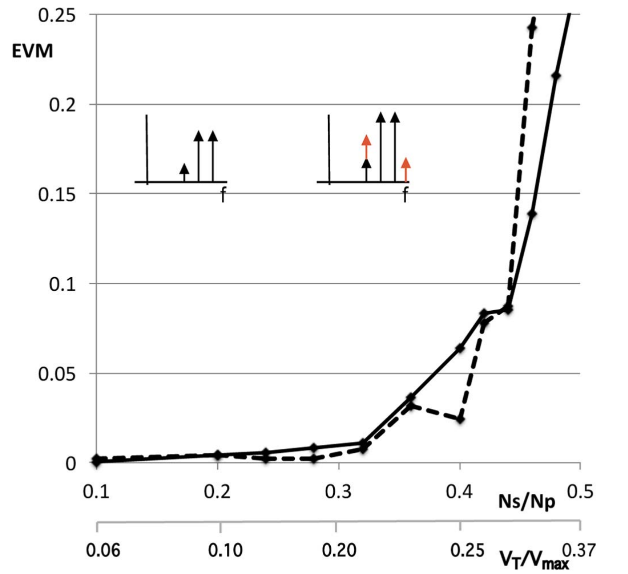

Fig. 3. EVM of the message versus fraction of samples retained. Message signal was a single-tone -80-dBm tone at 240 MHz. The interferer was two tones at {270, 300} MHz with amplitudes $\{0.011, -j * 0.011\}$ (dashed line) corresponding to a total average power of -26 dBm. The relative phases of the interferers were incremented by 45° five times and the resulting six EVMs averaged (solid line). Left inset illustrates sample amplifier input, and right inset illustrates how third-order sidebands mask the message.

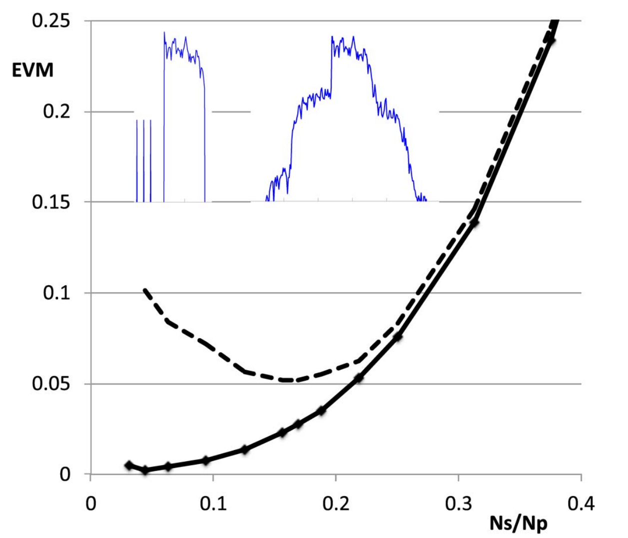

Fig. 4. EVM of the message versus fraction of samples retained. Message signal has three tones of normalized amplitude $\{1, j, -1\}$ at frequencies of {293, 294, 295} MHz, with a total power of -80 dBm. The interferer was an 8VSB random sequence at 297–303 MHz, with a total power of -8 dBm. IIP3 = 10 dBm. 100 sequences of $T_{\mathrm{dur}} = 8\ \mu$s were averaged. Solid line: no noise. Dashed line: with -95-dBm noise and 20-MHz bandwidth centered at 300 MHz. Left inset illustrates sample amplifier input spectrum (log amplitude). Right inset shows corresponding output when *no samples discarded*; distortion masks message.

drops below 10%, when the smallest 4500 of the overall 16 000 samples are used in the algorithm.

When the number of samples becomes very small, the condition number of $\mathbf{A}$ becomes large and the solution becomes sensitive to noise. To investigate the effect of noise, we added a band-limited normally distributed noise signal to the input of our model amplifier. A different realization of the noise was added to each of the 100 realizations of the interferer used in Fig. 4. The EVM results were averaged to produce the dashed line in Fig. 4. With noise, the EVM reaches a minimum as the number of samples is reduced (V_T decreasing) and then increases due to the poorer conditioning. This is the major factor limiting how large an interferer (or how low a V_T/V_{MAX}) can be tolerated.

IV. Formulation: Unknown Interferer Spectrum

A. Expansion With Subdomain Functions

In the previous examples, it was assumed that the interferer and message frequencies are known precisely and then used in the expansion (3). Usually, a receiver will not know the exact frequencies of an interferer. The LMS fit in (5) is sensitive to the assumed spectrum and cannot extract a small message when there are even small errors in the assumed spectrum.

To remedy this problem, we assume a set of N_{fI} expansion sinusoids with frequencies that span the interference spectrum. To accommodate the possibility that the expansion frequencies do not match up with the interferer's spectrum, we suppose a modulation of the complex amplitude of each expansion sinusoid. The modulation is approximated by a series of overlapping triangle functions (a type of linear spline) that span the sample record.

We divide the duration of the sample record T_{dur} into N_{seg} segments of equal length, i.e., $T_{\mathrm{seg}} = T_{\mathrm{dur}}/N_{\mathrm{seg}}$. An expansion triangle is centered at the boundaries between each segment. This leads to the following expansion of the interferer:

$$v_{\mathrm{oE}}(t_m) = c_o + \sum_{n=1}^{N_{fI}} \sum_{i=0}^{N_{\mathrm{seg}}} \mathrm{Re}\left[c_{ni}\mathrm{tr}(t_m - iT_{\mathrm{seg}})e^{j\omega_n t_m}\right] + \sum_{n=1}^{N_{fM}} \mathrm{Re}\left[c_{nM}e^{j\omega_{Mn} t_m}\right] \quad (6)$$

where $\mathrm{tr}(\tau) = 1 - |\tau|/T_{\mathrm{seg}}$ for $|\tau < T_{\mathrm{seg}}$ and zero otherwise. Thus, each triangle function covers two segments and overlaps its neighbors. (The endmost functions extend beyond the sample record, but are never evaluated there.) The constant $c_{ni} = c_{Rni} + jc_{Ini}$ is the amplitude at the boundary between the $i-1$ and ith time segments for the nth frequency. The interferer is thus determined by a set of $2(N_{\mathrm{seg}}+1)N_{fI}$ real coefficients.

Presumably, the message can be expressed in some set of known frequencies $\{\omega_{Mn}\}$, and no subdomain modulations are necessary. The message is fit by N_{fM} complex constants $c_{nM} = c_{RnM} + jc_{InM}$, where $n = 1, 2, \ldots, N_{fM}$.

The unknowns in (6) form a vector $\mathbf{x} = [c_0, c_{R11}, c_{R12}, \ldots, c_{R21}, c_{R22}, \ldots, c_{RM1}, c_{RM2}, \ldots, c_{I11}, c_{I12}, \ldots, c_{I21}, c_{I22}, \ldots, c_{IM1}, c_{IM2}, \ldots]$ of length $1 + 2(N_{\mathrm{seg}}+1)N_{fI} + 2N_{fM}$. As in the previous section, (6) can be written as a matrix equation $\mathbf{v}_{\mathrm{oE}} = \mathbf{F}\cdot\mathbf{x}$, where $\mathbf{F}$ now has dimensions $M_I \times [1 + 2(N_{\mathrm{seg}}+1)N_{fI} + 2N_{fM}]$. $\hat{\mathbf{x}}$ is determined by LMS best fit, as in the previous section. The N_{fM} complex message coefficients $\hat{c}_{nM}$ can be retrieved from $\hat{\mathbf{x}}$ and used to calculate EVM in the examples that follow.

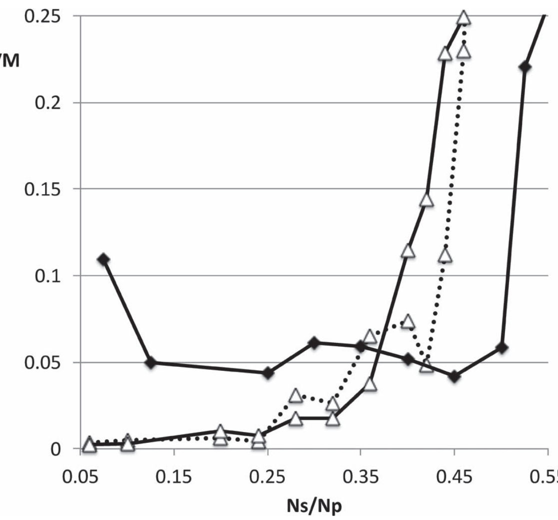

Fig. 5. EVM of the message versus fraction of samples retained, when interferer frequencies do not fall on the assumed expansion support, and subdomain modulation expansion is necessary. Message signal: single tone with −73-dBm power. Amplifier IIP3 is −9 dBm, $f_s = 2$ GHz, $T_{\mathrm{dur}} = 4\ \mu$s, $T_{\mathrm{ADC}} = 4$ ns. Interferer: two equal magnitude tones with a total average power of −26 dBm. Case I (♦): interferers at {297.4, 300.6} MHz with expansion frequencies from 297 to 302.6 MHz, with 0.8-MHz spacing and $N_{\mathrm{seg}} = 6$. Case II (△): interferers at {297.6, 300.4} MHz with expansion frequencies from 297 to 303 MHz, with 0.4-MHz spacing and $N_{\mathrm{seg}} = 2$. Solid lines are averages over six different interferer relative phases. Dashed line is for 45° relative phase between interferers.

B. Simulated Results: Unknown Interferers

The EVMs of the first two examples are plotted in Fig. 5. In those examples, the interferer consists of two tones with equal magnitude, but different relative phase (see caption). A single-tone message signal is located at a frequency where it is covered by the third-order intermodulation of the interferer tones. We chose expansion frequencies that span 297–303 MHz and plotted results for two different densities. The interferer frequencies are chosen for a worst case scenario, where the unknown interferers happen to be located between the expansion frequencies.

As in the previous results, Fig. 5 shows that the error increases when more distorted samples are included. The EVM curves vary as sample times redistribute when the relative interferer phase changes. The solid lines show results, where each point is an average of five EVMs taken as the interferer relative phase increments by 45°. The dashed line is the one member of that set that corresponds to an interferer relative phase of 45° (useful for verification.)

The better results occur when the expansion frequencies are more densely spaced (40-MHz spacing, $N_{fI} = 15$); only three triangle functions ($N_{\mathrm{seg}} = 2$) are necessary for good performance. When a less dense set of expansion frequencies are chosen (80-MHz spacing, $N_{fI} = 8$), the EVM becomes sensitive to the number of segments used. For the less dense set, the curve plotted in Fig. 5 corresponds to $N_{\mathrm{seg}} = 6$. Using 8 segments gave similar results while using 7 segments produces much better results.

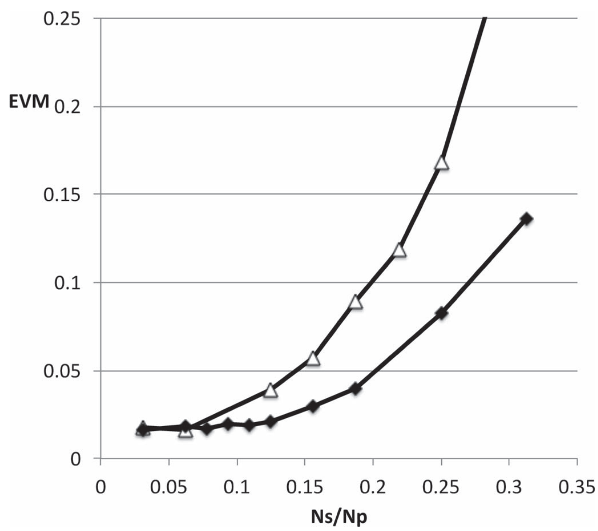

Fig 6. EVM of the message versus fraction of samples retained when 8VSB interferer frequencies do not fall on the assumed expansion support. Message signal was three tones of amplitude $\{1, j, -j\}$ at frequencies of {293, 294, 295} MHz, with a total power of -73 dBm. The interferer was an 8VSB random sequence at frequencies of 297.0325–303.0325 MHz, with a total power -8 dBm. Expansion frequencies from 297 to 303 MHz, with 0.5-MHz spacing; $T_{\rm seg} = 1$ μs. 100 sequences were averaged for each point. Block lengths are $T_{\rm dur} = 8$ μs ($\triangle$) and 16 μs ($\blacklozenge$).

Fig. 6 shows EVM results where the 8VSB interferer described in Fig. 4 is centered at 300.0325 MHz. Twelve expansion frequencies are chosen from 297 to 303 MHz, none of which fall on the tones that make up the test signal. A message signal represented by three tones is located at [293, 294, 295] MHz, where the complex amplitude of each tone remains constant over the sample record. Each EVM point on the plot is the average of 100 interferer symbol sequences. For the 8-μs record, the number of subdomain expansion functions was $N_{\rm seg} = 8$, while the 16-μs record used double that, i.e., $N_{\rm seg} = 16$. The longer record gave lower EVM since there are double the number of samples retained.

V. Discussion

The previous examples suggest that a weak message signal can be extracted even when accompanied by very large interferers and first amplified by a device with realistic nonlinearity. The success of the extraction relies on 1) selecting a sufficient number of undistorted samples, 2) accurate knowledge of the message spectral support, or 3) using a flexible expansion to fit the interferer.

Consider the DTV-related example described in Fig. 4. Additional simulations of that example show that, if all samples were accepted and EVM were plotted versus amplifier IIP3 for the parameters in Fig. 4, the amplifier IIP3 would need to be greater than 28 dBm in order to reduce the sideband shoulders enough to get an EVM less than 10%. Such a linear LNA is a heroic achievement. In contrast, the IIP3 necessary for the results in Fig. 4 is 10 dBm, an achievable amplifier that requires much less dc power.

In the algorithms described, the complex amplitude of a message is recovered by LMS fitting a set of expansion functions to a set of retained samples. When fewer samples are retained, the accuracy of message retrieval becomes sensitive to noise, and this limits the degree to which the time-selective sampling approach can ameliorate the effects of a nonlinearity. Noise can be generated in the conventional sense, but if the expansion functions do not sufficiently cover the signal space of the interferer, then the uncovered interferer also acts as noise in the LMS fit. Thus, the fitting method described in Section IV is critical in cases where the interferer support is not well known. Further algorithm development should improve conditioning and reduce sensitivity to noise.

The simple cubic model of the LNA used in this brief assumed no memory effect. The measurements described in [3] show no evidence of this effect, but they did not measure very low-level signals. Simulations not included here show that to minimize memory effects the amplifier must have a large bandwidth, but not unreasonably large for current technology.

This brief shows how an RF sampling receiver could be designed to mitigate the effects of amplifier nonlinearity when large interferers are present. The concept eliminates the need for reconfigurable filters prior to low-noise amplification. The algorithm and associate parameters (such as sampling and ADC speed) are reasonable for implementation in current CMOS technology.

Acknowledgment

The author would like to thank Prof. D. Goeckel, Prof. M. Duarte, and Dr. A. Polak for helpful discussions.

References

[1] C. Stevenson *et al.*, "IEEE 802.22: The first cognitive radio wireless regional area network standard," *IEEE Commun. Mag.*, vol. 47, no. 1, pp. 130–138, Jan. 2009.

[2] S. J. Shellhammer, A. K. Sadek, and W. Zhang, "Technical challenges for cognitive radio in the TV white space spectrum," in *Proc. Inf. Theory Appl. Workshop*, San Diego, CA, USA, Feb. 2009, pp. 323–333.

[3] R. W. Jackson and M. Shusta, "Interference rejection by time selective sampling," in *Proc. EuMC*, Nuremberg, Germany, Oct. 2013, pp. 573–576.

[4] J. S. Abel and J. O. Smith, "Restoring a clipped signal," in *Proc. ICASSP*, Toronto, ON, Canada, Oct. 1991, vol. 3, pp. 1745–1748.

[5] A. J. Weinstein and M. B. Wakin, "Recovering a clipped signal in sparseland," *Sampling Theory Signal Image Process.*, vol. 12, no. 1, pp. 55–69, 2013.

[6] A. Polak, M. F. Duarte, R. W. Jackson, and D. L. Goeckel, "Recovery of sparse signals from amplitude-limited sample sets," in *Proc. IEEE ICASSP*, Vancouver, BC, Canada, 2013, pp. 4663–4667.

[7] R. J. Martin and D. A. Castelow, "Reconstruction of multiband signals using irregular sampling," *GEC J. Technol.*, vol. 14, pp. 180–185, 1997.

[8] Y.-R. Sun and S. Signell, "Algorithms for nonuniform bandpass sampling in radio receiver," in *Proc. ISCAS*, 2003, pp. 1-1–1-4

[9] F. Marvasti and A. Amini, "Reconstruction of multiband signals from non-invertible uniform and periodic nonuniform samples using an iterative method," presented at the Sampling Theory Applications, Thessaloniki, Greece, 2007.

[10] K. Gröchenig, "Reconstruction algorithms in irregular sampling," *Math. Comput.*, vol. 59, no. 199, pp.181–194, 1992.

[11] F. Marvasti, *Nonuniform Sampling: Theory and Practice*. New York, NY, USA: Springer-Verlag, 2001.

[12] M. Ben-Romdhane, C. Rebai, A. Ghazel, P. Desgeys, and P. Loumeau, "Non-uniform sampling schemes for IF sampling radio receiver," in *Proc. Int. Conf. DTIS*, Tunis, Tunisia, Sep. 2006, pp. 15–20.

[13] A. Maalej, C. Rebai, M. Ben-romdhane, and A. Ghazel, "Pseudo-random direct sampler for frequency down-conversion in a multi-standard receiver," in *2nd Int. Conf. SCS*, Monastir, Tunisia, Nov. 2008, pp. 1–6.

[14] M. Wakin *et al.*, "A nonuniform sampler for wideband spectrally sparse environments," *IEEE J. Emerging Sel. Topics. Circuits Syst.*, vol. 2, no. 3, pp. 516–529, Sep. 2012.